Fe-assisted hydrothermal liquefaction of cellulose: Effects of hydrogenation catalyst addition on properties of water-soluble fraction

Hirano, Yoshiaki ; Miyata, Yoshinori ; Taniguchi, Makiko ; Funakoshi, Nami ; Yamazaki, Yoshiko ; Ogino, Chiaki ; Kita, Yuichi

(Citation)
Journal of Analytical and Applied Pyrolysis,145:104719

(Issue Date)
2020-01

(Resource Type)
journal article

(Version)
Accepted Manuscript

Fe-assisted hydrothermal liquefaction of cellulose: Effects of hydrogenation catalyst addition on properties of water-soluble fraction

Yoshiaki Hirano,[a*] Yoshinori Miyata,[a,b] Makiko Taniguchi,[a] Nami Funakoshi,[a] Yoshiko Yamazaki,[a] Chiaki Ogino,[a] and Yuichi Kita[a]

[a]*Department of Chemical Science and Engineering, Graduate School of Engineering, Kobe University, Kobe 657-8501, Japan*

[b]*Research Center, Innovation & Business Development Division, Nippon Shokubai Co., Ltd., Suita, Osaka 564-8512, Japan*

[*]Corresponding author. Tel.: +81-78-803-6512, email: hirano@phoenix.kobe-u.ac.jp

Abstract

Hydrothermal liquefaction (HTL) is an effective way of converting biomass into fuels and chemicals. Recently, the addition of catalysts in the HTL has been investigated to improve the yield and quality of bio-oil. We previously reported that metallic-Fe-promoted HTL of lignocellulosic biomass affords a water-soluble (WS) fraction that furnishes light olefins and aromatic hydrocarbons upon catalytic cracking over a solid acid catalyst. We demonstrated that the Fe-assisted HTL of cellulose in the presence of a hydrogenation catalyst results in a superior yield and quality of the WS fraction, thereby enhancing the hydrocarbon yield in the catalytic cracking of the WS fraction. When the HTL of cellulose was performed in the presence of Fe and Pd/Al_2O_3 at 250 °C for 1 h, the WS fraction yield reached 73%. The addition of hydrogenation catalysts led to higher hydrogen-to-effective-carbon ratios (up to 1.33) and proportions of the volatile light WS fraction (up to 63%) than those obtained by Fe-assisted HTL. This improved performance was attributed to the synergistic acceleration by metallic Fe and the hydrogenation catalyst, which particularly hydrogenates ketones to alcohols. Finally, a plausible mechanism that explains the effect of the hydrogenation catalyst was proposed.

Keywords: hydrothermal liquefaction, cellulose, metallic iron, hydrogenation catalysts, water-soluble fraction, catalytic cracking

Introduction

Biomass features the advantages of renewability, carbon neutrality, and high energy potential, and is therefore a promising fossil-resource substitute [1–7]. Consequently, numerous biochemical (fermentation) and thermochemical (gasification, pyrolysis, and hydrothermal liquefaction (HTL)) processes have been developed for the conversion of biomass into fuels and chemical feedstocks. In particular, HTL, which is a promising method for converting energy-rich biomass into bio-oil and is carried out in aqueous media at moderate temperatures (280–370 °C) and high pressures (10–25 MPa), does not require energy-intensive dewatering/pre-drying steps and is thus suitable for substrates with relatively high moisture contents [8–17]. Typically, the HTL of biomass affords four fractions, namely the water-soluble (WS) fraction, the water-insoluble (WI) fraction (bio-oil or biocrude), solid residue (char), and gases. Bio-oil obtained by HTL is rich in oxygenated compounds and therefore cannot be directly used in oil refineries, requiring upgrading before use as a fuel or chemical feedstock.

Both homogenous and heterogeneous catalysts have been employed to improve the yield and quality of HTL-produced bio-oil [18–32]. For instance, homogeneous catalysts such as inorganic acids (H_3PO_4, $HCOOH$, CH_3COOH, $HClO_4$, HCl, and H_2SO_4) and alkalis (Na_2CO_3, $NaOH$, K_2CO_3, KOH, and $Ca(OH)_2$) suppress char formation and enhance the yield of bio-oil, although they do not have any effect on bio-oil quality. In contrast, metals (Pt, Pd, Ru, Ni, and Co) as heterogeneous hydrogenation catalysts and metal oxides (MgO, Al_2O_3, CaO, MnO, NiO, CuO, ZnO, ZrO_2, SnO, La_2O_3, CeO_2, zeolites, and mixed oxides) as heterogeneous solid acid-base catalysts can improve both the yield and quality of bio-oil. The improvement in bio-oil quality in the presence of heterogeneous catalysts has been ascribed to their promotional effects on dehydration, decarbonylation, decarboxylation, hydrogenation, and hydrogenolysis reactions. However, as the choice of catalyst depends on the biomass feedstock and reaction conditions, further studies are needed to identify catalysts suitable for achieving the desired yield and quality of bio-oil produced by biomass HTL and to elucidate the mechanism associated with this quality improvement [15].

From the viewpoint of making the whole HTL process commercially feasible, the use of the biomass-HTL-produced WS fraction has attracted little attention [33]. Although the WS fraction produced by biomass HTL has not been extensively investigated, several studies on its anaerobic digestion [34], gasification [35], ketonization [36], and hydroprocessing [37] have been reported. Recently, we demonstrated that when the HTL of lignocellulosic biomass is performed in the presence of metallic Fe powder, char formation is dramatically suppressed, and the yield of the WS fraction is significantly increased. Moreover, the catalytic cracking of the thus produced WS fraction over a zeolite catalyst affords high amounts of light olefins and BTX (benzene, toluene, and xylene) as basic chemicals [38]. We also investigated the HTL of cellulose, hemicellulose, and lignin as model lignocellulose substrates and proposed an overall reaction pathway for the Fe-assisted HTL of lignocellulosic biomass [39], suggesting that metallic Fe and in situ generated Fe oxides synergistically promote the formation and hydrogenation of light compounds in the WS fraction. However, in order for biomass HTL to be economically viable, the usage efficiency of the system (reducing capacity of metallic iron) needs to be improved so that the yield and quality of the WS fraction are further enhanced, and a plausible HTL mechanism needs to be elucidated.

Herein, we investigated the effects of heterogeneous metal catalysts (Pd, Pt, Ru, Co, Ni, and Cu) on the yield and quality (e.g., hydrogen-to-effective-carbon ratio (H/C_{eff}) and the proportion of volatiles) of the WS fraction produced by Fe-assisted HTL of cellulose. Moreover, we examined the conversion of the thus obtained WS into light olefins (ethylene, propylene, butene) and BTX by catalytic cracking and proposed a plausible explanation of the beneficial effect of hydrogenation catalysts on the yield and quality of the WS fraction.

2. Experimental

2.1. Materials

Cellulose (Avicel® PH-101) was purchased from Sigma-Aldrich Co., LLC. Fe powder (99.9%, NM-0029-UP) was purchased from Ionic Liquids Technologies GmbH (Germany). Noble metal–based hydrogenation catalysts (5 wt%-Pd/ Al_2O_3, 5 wt%-Pt/ Al_2O_3, 5 wt%-Ru/Al_2O_3) were purchased from N.E. CHEMCAT Corporation (Japan) and used as received. Transition metal–based hydrogenation catalysts, namely stabilized Ni (SN-250, 56 wt%-Ni/kieselguhr) and Cr-free Cu (KC-1, 48 wt%-CuO/CaO/SiO_2) were supplied by Sakai Chemical Industry Co., Ltd. (Japan). The catalytic cracking catalyst (HZSM-5 zeolite with a Si/Al molar ratio of 24:1) was supplied by Nippon Shokubai Co., Ltd. (Japan). Oxidized Fe (FeO_x) was prepared by thermal treatment of Fe powder (6.256 g) in water at 250 °C for 1 h, as described in the next section.

2.2. HTL process and HTL product analysis

Cellulose was liquefied and fractionally separated as described in our previous study [38]. Typically, cellulose (4.000 g), Fe powder (0 or 6.256 g), metal catalyst (0.400 g, 0.02 g in metal equivalent), and water (40 g) were loaded into a 100-mL autoclave equipped with an electric heater and an electromagnetic inductive agitator. The autoclave was purged with N_2 for four times to remove air, and the initial pressure (N_2) was set to 1.0 MPa. The reactor was rapidly heated to 250 °C at ~20 °C/min, maintained at this temperature for 1 h at a stirring speed of 700 rpm, and then rapidly cooled to 25 °C by immersion in an ice-water bath. Gaseous products were collected in a gas sampling bag, and WS products were isolated by filtration of the reaction mixture slurry. The filter cake was extracted with acetone, and the extract was concentrated via rotary evaporation at reduced pressure (60 °C, 1 h) to afford the WI fraction. The solid residue (SR) collected by filtration was dried at 70 °C at reduced pressure overnight and weighed. Product yields and properties were determined by previously reported methods [38]. A total organic carbon analyzer (Shimadzu, TOC-$L_{CSH/CSN}$) was employed to determine the yield of the WS fraction. Elemental analysis (CHN; Elementar, Vario EL cube) was performed to determine the carbon contents of the WI fraction and the SR. Gaseous products were analyzed using a gas chromatograph (Shimadzu, GC-8A) equipped with silica-gel, 5-Å-molecular-sieve columns, and a thermal conductivity detector (TCD).

The yields of HTL-produced fractions were calculated as

$$\text{Yield (\%)} = \frac{\text{Moles of carbon in the fraction}}{\text{Moles of carbon in loaded cellulose}} \times 100. \qquad (1)$$

2.3. Evaluation of WS fraction quality

The quality of the WS fraction (H/C_{eff} ratio and proportion of volatiles) was evaluated by previously reported methods [40]. A gas chromatograph (Shimadzu, GC-2014) equipped with a flame ionization detector (FID) and a capillary column (GL Sciences, Inert-cap® WAX-HT, 30 m × 0.25 mm ID × 0.25 µm film thickness) was used to calculate the concentration of each constituent in the WS fraction, and the H/C_{eff} ratio was determined in accordance with Eq. 2.

$$\mathrm{H/C_{eff}} = \frac{[\mathrm{H}] - 2[\mathrm{O}]}{[\mathrm{C}]} \quad (2).$$

Here, [H], [O], and [C] represent the total contents of hydrogen, oxygen, and carbon, respectively, in the bio-oil, which were quantified by GC analysis. The relative contents of light and heavy components in the crude WS fractions were determined by a freeze-drying method.

2.4. Catalytic cracking and cracking product analysis

The WS fraction was catalytically cracked in a fixed-bed continuous-flow reactor following a previously reported method [38]. Prior to cracking, the reactor was loaded with HZSM-5 (6.0 mL) and heated at 600 °C for 1 h under a flow of N_2 (50 mL/min). The WS fraction was fed into the reactor at a weight hourly space velocity of 1.1 h^{-1} and a temperature of 600 °C. During the reaction, condensable and non-condensable gaseous products were collected for 120 min using gas wash bottles and gas sampling bottles, respectively. Two gas chromatography systems, equipped with a TCD or an FID, were employed to quantify CO_2, CO, alkanes (C_1–C_5), light olefins (ethylene, propylene, and butene), and BTX (benzene, toluene, and xylene).

The yields of the catalytic cracking products were calculated using:

$$\text{Yield (\%)} = \frac{\text{Moles of carbon in the product}}{\text{Moles of carbon in WS fraction fed in}} \times 100 \qquad (3).$$

The water-solubles yield was calculated from the content of the water-soluble species condensed in the gas wash bottle determined by total organic carbon analysis, minus the BTX carbon content. Catalyst coking was rarely observed, and the carbon balances were slightly deficient because of the carbonization of non-volatile compounds on the vaporizer in the reactor.

3. Results and discussion

3.1. Effect of the hydrogenation catalyst on the HTL of cellulose

Fe-assisted HTL was performed in the presence of various noble and transition-metal-based catalysts, and the product yields were compared to those obtained without a catalyst in the presence/absence of Fe (Fig. 1). The addition of a metal catalyst increased the yield of the WS fraction (except for the case of Fe + Ru/Al_2O_3) and decreased that of the WI fraction compared to the yields obtained by Fe-assisted HTL, while Fe-assisted HTL remarkably suppressed SR formation and increased the yield of the WS fraction. As has been reported previously [38], the increased yield of the WS fraction during Fe-assisted HTL is ascribed to the increased production of hydroxyketones via the retro-aldol condensation of sugars and the subsequent hydrogenation of the resulting aldehydes. Metallic Fe acts as a reductant in the hydrogenation of aldehydes [39]; however, Fe also reacts with water under hydrothermal conditions to generate hydrogen

($3Fe + 4H_2O \rightarrow Fe_3O_4 + 4H_2$). Because we confirmed that hydrogen in the gas phase did not affect the yields of HTL products [38], hydrogen generation decreases the reducing capacity of Fe in the case of Fe-assisted HTL. For the utilization of the metal hydrogenation catalyst in Fe-assisted HTL, we suggested that the added metal catalysts activate gas-phase hydrogen in order to form hydrogenate intermediate compounds in the WS fraction, thereby resulting in the efficient usage of in-situ-generated hydrogen, which could not have been available with Fe alone. Thus, metal catalysts are considered to accelerate the hydrogenation of in-situ-formed unstable aldehydes, increase the yield of stable hydroxyketones, and suppress the formation of condensation products (WI fraction), which boosts the WS fraction.

The GC profiles and compositions of WS fractions recorded/determined using previously reported methods [40] are shown in Fig. 2 and Table S1, respectively. A larger quantity of high-boiling volatile compounds was produced in the presence of Fe + Pd/Al_2O_3 than in the Fe-only case, while only few peaks were observed in the no-catalyst no-Fe profile. Fe-assisted HTL produced hydroxyketones such as 2-hydroxy-3-butanone, 1-hydroxy-2-propanone, and 1-hydroxy-2-butanone, while diol (ethylene glycol, propylene glycol, 2,3-butanediol, and 1,2-butanediol) formation was favored in the case of the Fe + Pd/Al_2O_3 system. Therefore, we recognized that hydroxyketones were hydrogenated to diols in the presence of Pd/Al_2O_3. Ethylene glycol, incidentally, was assumed to be formed via the hydrogenation of glycolaldehyde, which, however, could not be detected by GC analysis. The above results indicate that metal catalysts promote the hydrogenation of unstable intermediates by using the gas-phase hydrogen formed in situ during Fe-assisted HTL to inhibit WI formation and increase WS formation.

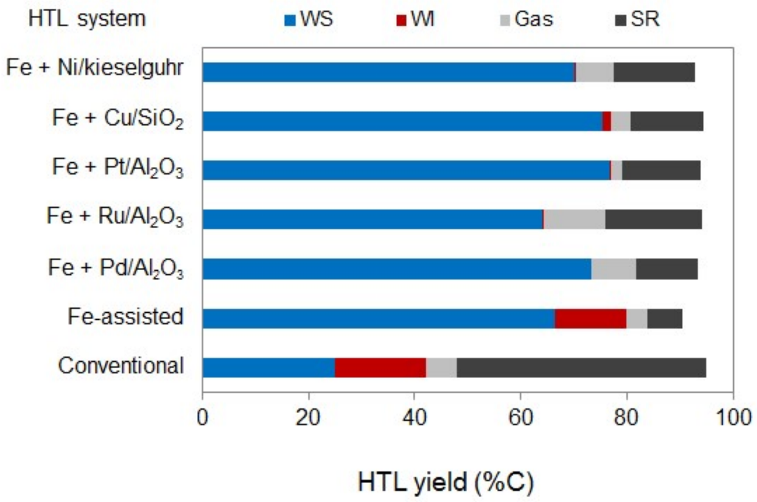

Fig. 1. Effects of hydrogenation catalysts on the Fe-assisted HTL of cellulose.

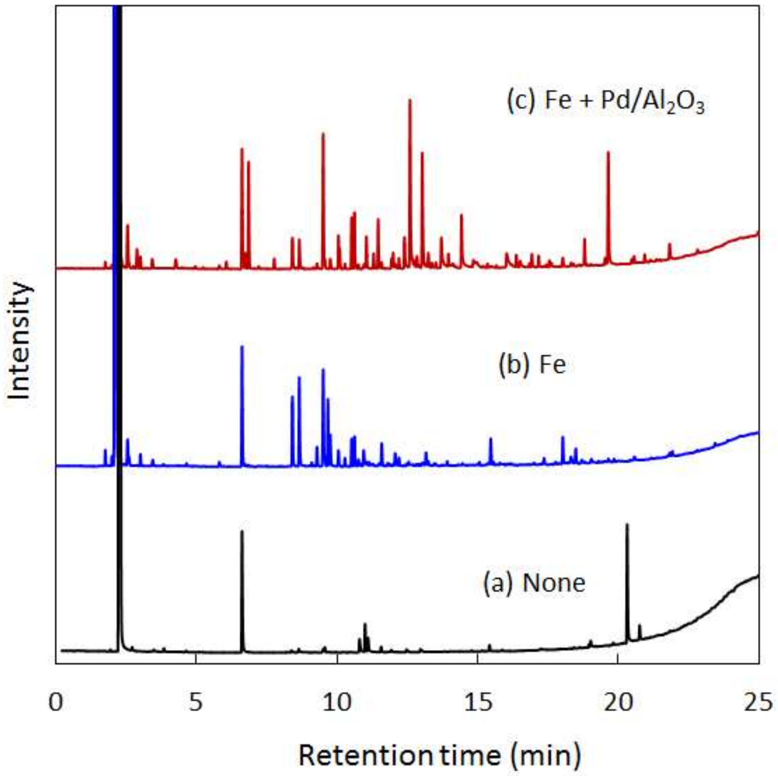

Fig. 2. GC profiles of WS fractions produced by cellulose HTL (a) in the absence of additives and in the presence of (b) Fe, and (c) Fe + Pd/Al$_2$O$_3$.

3.2. Effect of hydrogenation catalyst on WS fraction quality

The elemental compositions of light WS components were determined by summing the contents of the elements in all compounds quantified by GC and are expressed as H/C, O/C, and H/C_{eff} ratios (Table 1). The H/C_{eff} ratio is often used to describe the degree of biomass upgrading, with high H/C_{eff} values indicating efficient reforming [41]. Generally, bio-based feedstocks, such as lignocellulose and carbohydrates, have H/C_{eff} ratios of 0–0.5, while petroleum-based feedstocks exhibit values of 1.0–2.0. Thus, an H/C_{eff} ratio above 1.0 is the benchmark for biomass upgrading.

The H/C ratios of the light WS components obtained in the presence of the hydrogenation catalysts were equal to or higher than those obtained in the Fe-only case, while the corresponding O/C ratios were lower than those obtained in the Fe-only case. Consequently, H/C_{eff} ratios above 1.0 were obtained in the presence of the hydrogenation catalysts, with the maximal value (1.33) observed for Pd/Al_2O_3. These results suggest that hydrogenation catalysts can promote the hydrodeoxygenation of intermediates during the Fe-assisted HTL of cellulose and are effective for improving the quality of the WS fraction. Vispute et al. studied the two-step hydrodeoxygenation of the water-soluble fraction of pinewood bio-oil [37], showing that the upgrading of this fraction via hydrodeoxygenation over a Ru catalyst increased the H/C_{eff} ratio from 0.14 to 0.71. In contrast, our one-step Fe-assisted HTL with a hydrogenation catalyst improved the H/C_{eff} ratio from 0.30 (no additive) to 0.56 (Fe only) and 1.33 (Fe + Pd) and proved to be more valuable for upgrading the WS fraction than the above-mentioned two-step process. Hence, we inferred that the metal catalysts improved the quality of the WS fraction via the hydrodeoxygenation of intermediates during the Fe-assisted HTL of cellulose.

The relative contents of the light components in the WS fractions (calculated on the basis of the carbon content of freeze-dried crude WS fractions) notably increased when HTL was performed in the presence of a hydrogenation catalyst (Table 1), in agreement with the enhanced production of volatiles observed in this case by GC (Fig. 2 and Table S1). As we demonstrated that WS fractions rich in light components afforded light olefins in high yields upon catalytic cracking [40], we expect that the WS fractions obtained by Fe-assisted HTL with hydrogenation catalysts are suitable for producing light olefins via catalytic cracking.

3.3. Catalytic cracking of WS fractions

We catalytically cracked the WS fractions obtained by the Fe-assisted HTL of cellulose with various hydrogenation catalysts (Fig. 3). The major products were light olefins (ethylene, propylene, and butene), along with minor products such as BTX, alkanes, and CO_x (CO and CO_2).

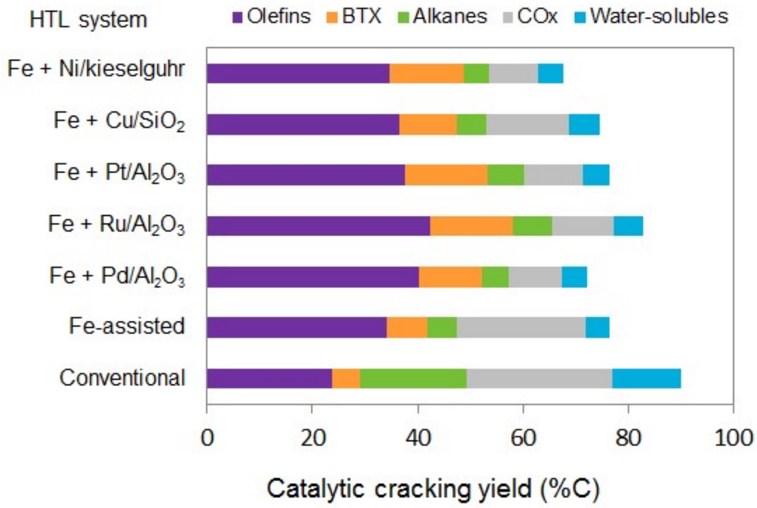

Fig. 3. Effect of added catalyst on the catalytic cracking of WS fractions obtained by Fe-assisted HTL of cellulose.

WS fractions obtained by Fe-assisted HTL in the presence of hydrogenation catalysts featured catalytic cracking yields higher than those observed for conventional or Fe-assisted HTL; e.g., the yields of olefins obtained using Pd or Ru catalysts (>40%) exceeded that (34%) obtained for the Fe-only case. Furthermore, the addition of a hydrogenation catalyst increased the yield of BTX. As a consequence, the total yield of hydrocarbons produced by HTL/catalytic cracking was 42% for the Fe + Pd/Al_2O_3 and Fe + Ru/Al_2O_3 systems, while a value of only 32% was observed for the Fe-only system.

To be suitable for biomass upgrading processes, such as catalytic cracking, bio-based feedstocks with high H/C_{eff} ratios are preferred [42]. As described in section 3.2, the H/C_{eff} ratios of the light WS components obtained by Fe-assisted HTL in the presence of hydrogenation catalysts were higher than those of light WS components obtained by Fe-assisted HTL in the absence of a catalyst (Table 1). As expected, components with higher H/C_{eff} ratios were more efficiently converted into hydrocarbons during catalytic cracking (Fig. 3), with the highest H/C_{eff} ratio and total hydrocarbon yield observed for the Pd/Al_2O_3 catalyst. A proportionate relationship exists between the H/C_{eff} ratio and catalytic cracking yield, in particular, the olefin and BTX yields of the WS fractions (Fig. S1).

According to the results for the Fe-assisted HTL of lignocellulose [40], the WS fraction obtained by Fe-assisted HTL with a hydrogenation catalyst exhibited a higher olefin yield than that obtained by conventional or Fe-assisted HTL, due to the increased content of light components in the former fraction (Table 1). Actually, the content of light components was further increased upon the introduction of a hydrogenation catalyst; e.g., WS fractions obtained in the presence of Pt and Ru catalysts featured light component contents almost twice as high as that of the WS fraction obtained in the Fe-only case. A proportional relationship exists between the content ratio of light WS fractions and the catalytic cracking yield of the WS fractions (Fig. S2), reconfirming that the hydrocarbon yield of the catalytic WS fraction cracking can be effectively increased by increasing the content of the light components in this fraction [40].

These results indicate that the catalytic cracking of the WS fraction is influenced by the hydrodeoxygenation degree of the WS component and the relative content of the light components in the WS fraction.

3.4. Plausible mechanism for hydrogenation catalyst effect

To determine the role of the hydrogenation catalyst in the Fe-assisted HTL of cellulose, we probed various

(Fe species + Pd/Al_2O_3) HTL systems (Fig. 4), investigated the catalytic cracking of the thus obtained WS fractions (Fig. 5), and evaluated their quality (Table 2). The GC profiles and compositions of the thus obtained WS fractions are presented in Figure S3 and Table S1, respectively.

As described above, the addition of Pd/Al_2O_3 to the Fe-containing system increased the WS fraction and cracking yields relative to those observed for the conventional HTL (no additive) and Fe-assisted (Fe alone) HTL systems due to the hydrogenation of unstable intermediates and the improvement of the WS fraction quality. When HTL was performed in the presence of Pd/Al_2O_3 alone (no Fe) under a hydrogen atmosphere equivalent to that used in the Fe-assisted HTL, the WS yield was slightly higher than that of the Fe + Pd/Al_2O_3 system. In this instance, hydroxyacetone was detected in a yield of 20.5% as a primary product (Table S1). Therefore, we infer that the Pd catalyst hydrogenates unstable intermediates formed during the hydrothermal reaction into stable compounds such as hydroxyketones to suppress condensation and re-polymerization, and enhance the WS fraction yield. On the other hand, the quality of the thus obtained WS fraction was lower than that obtained in the case of the Fe + Pd/Al_2O_3 system (Table 2) so that the catalytic cracking yield was lower than that of the Fe + Pd system. The H/C_{eff} ratio and light component content of the WS fraction (0.82 and 52%, respectively) by the Pd/Al_2O_3 + H_2 system were intermediate between those obtained for Fe-assisted (0.56 and 36%, respectively) and Fe + Pd/Al_2O_3 (1.33 and 63%, respectively) systems. FeO_x alone resulted in an exceptionally low yield of the WS fraction. The FeO_x + Pd/Al_2O_3 + H_2 system led to a high yield of the WS fraction in the HTL and hydrocarbons during catalytic cracking, although the yields were less than those of the Fe + Pd/Al_2O_3 system. This implies that

Fe and Pd/Al_2O_3 act synergistically to improve the WS fraction quality by promoting the hydrogenation of intermediates, thereby increasing the catalytic cracking efficiency. This is supported by the fact that the HTL with the Fe or $Pd/Al_2O_3 + H_2$ system only afforded hydroxyacetone, while the Fe + Pd/Al_2O_3 system sequentially hydrogenated to produce propylene glycol (Table S1). We speculate that the Fe species activate the carbonyl group of the hydroxyacetone molecule to enable the Pd catalyst to hydrogenate it to propylene glycol, as discussed in our previous study [43].

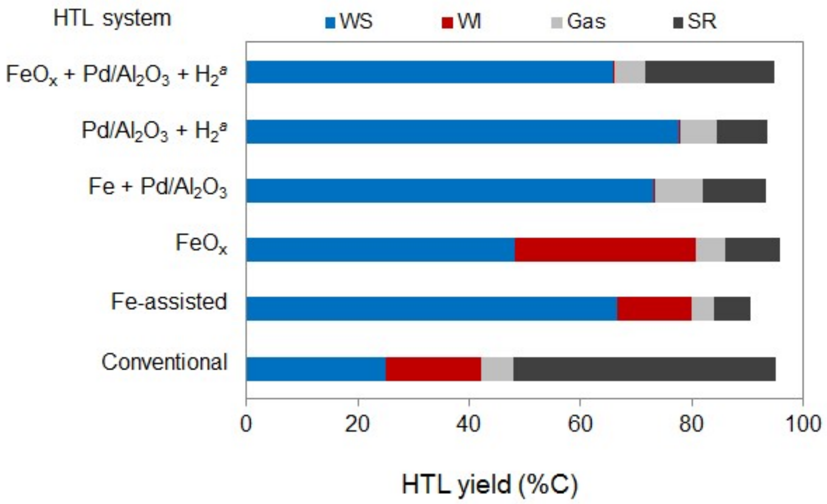

Fig. 4. Effects of the Fe additive and Pd catalyst on cellulose HTL.

[a]Initial pressure = 1.0 MPa N_2 + 1.5 MPa H_2 (i.e., the atmosphere was identical to that used for Fe-assisted HTL).

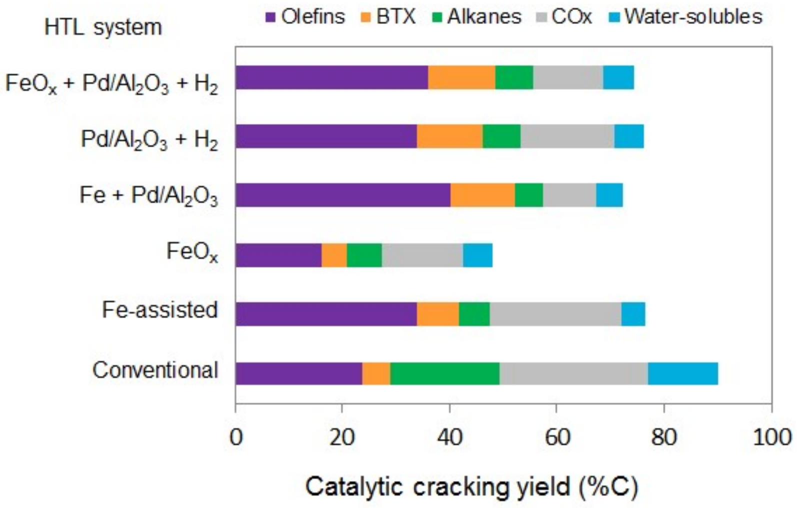

Fig. 5. Effects of the HTL system on the catalytic cracking of WS fractions.

Based on the above results and our previous findings [38, 39, 43, 44], in this study we propose a plausible mechanism to explain the effect of the hydrogenation catalyst on the overall HTL reaction pathway (Scheme 1). In this mechanism, cellulose is rapidly hydrolyzed to glucose, which reversibly isomerizes into fructose. The retro-aldol condensation of the (glucose + fructose) mixture catalyzed by FeO_x affords C_2–C_4 intermediates, such as erythrose, glycolaldehyde, dihydroxyacetone, and glyceraldehyde. At this point, it is worth noting that FeO_x species are assumed to promote the retro-aldol and isomerization reactions on the basis of our previous studies on the transformation of glucose to C_3 chemicals such as hydroxyacetone, propylene glycol, and lactic acid under hydrothermal conditions [43, 44]. In the absence of Fe, the unstable C_2–C_4 intermediates easily undergo isomerization (keto-enol tautomerization), dehydration, condensation, and carbonization to afford oligomers, polymers, and char as the WI fraction or SR components [45]. Contrastingly, metallic Fe and Pd catalyze the hydrogenation of these aldehydes into stable alcohols under hydrothermal conditions to increase the WS fraction yield. As described above, a Pd catalyst activates gas-phase hydrogen derived from the reaction of Fe with water so as to effectively boost the hydrogenation of intermediate compounds, while metallic Fe stabilizes unstable intermediates by an electron-transfer-type reduction [39]. Finally, a key finding in this study is that the reduction of intermediates was dramatically accelerated by the contributions of both the metallic Fe and the Pd catalyst. Moreover, Pd catalysts can additionally hydrogenate ketones into alcohols in cooperation with Fe, which is aided by the activation of the carbonyl group, to improve the quality of the WS fraction. In agreement with the suggested mechanism, numerous diols (ethylene glycol, propylene glycol, 2,3-butanediol, 1,2-butanediol, 1,2-pentanediol, and 1,2-hexanediol) were formed in the Fe + Pd/Al_2O_3 system (Table S1). Studies on the non-catalytic and catalytic HTL of various biomasses [1–5, 8–32] demonstrated that the HTL process can be divided into three steps, namely depolymerization, decomposition, and re-polymerization (condensation). However, as biomass is a complex mixture of carbohydrates, lignin, proteins, and lipids, the exact mechanism of HTL has not yet been elucidated, with only few studies dealing with the effect of Fe powder on biomass HTL [46, 47]. Chen et al. showed that a conversion of 89.45 wt% (sum of heavy bio-oil and aqueous product yields; 270 °C, 30 min) was achieved when wheat stalk liquefaction was performed in the presence of Na_2CO_3 and Fe, and probed the compositions of heavy bio-oil and the WS fraction by GC-MS. de Caprariis et al. demonstrated the effect of Fe powder addition on the HTL of oak wood, revealing that the use of Fe not only increased the yields of bio-oil, but also improved its quality by facilitating the in situ formation of H_2. However, neither of the two abovementioned studies proposed a detailed mechanism. The present work suggests a plausible mechanism for cellulose liquefaction to afford the WS fraction and therefore helps to unfold the mechanism of HTL and to speculate how the WS fraction is sequentially converted into the WI fraction (biocrude) and SR (char) when hydrogenation catalysts are used.

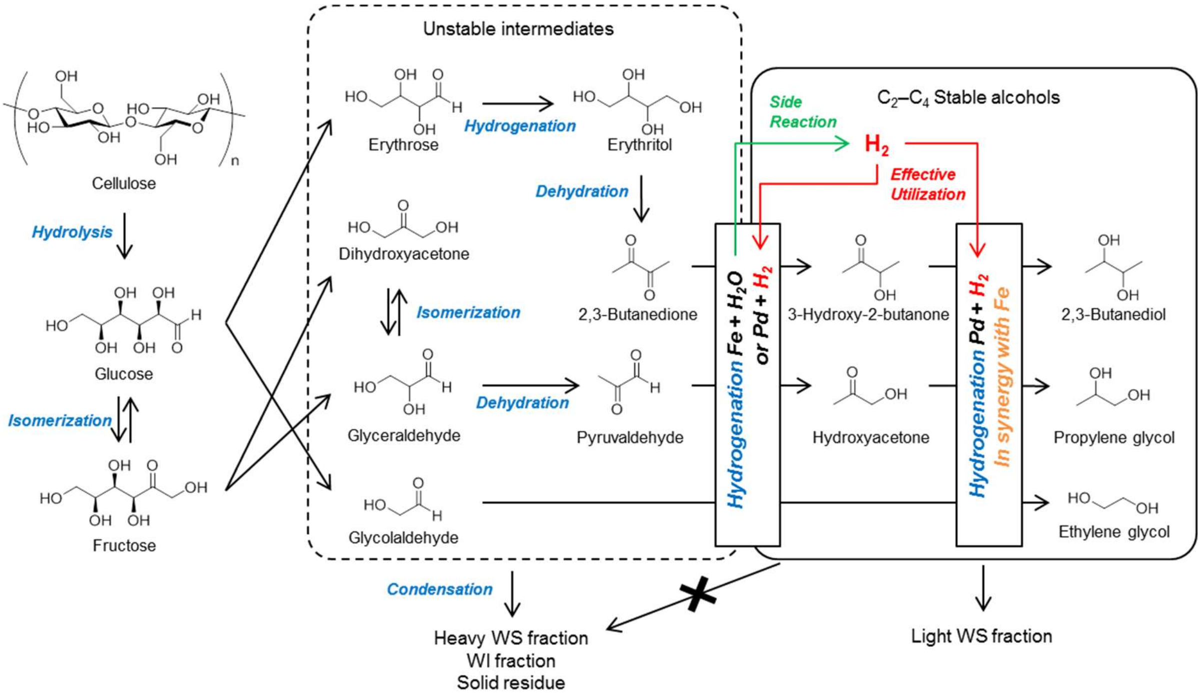

Scheme 1. Plausible mechanism for the effect of Pd catalysts on the Fe-assisted HTL of cellulose.

4. Conclusion

The addition of metal hydrogenation catalysts increased the yield and quality of the WS fraction formed in the Fe-assisted HTL of cellulose and facilitated the efficient conversion of this fraction into light olefins and aromatics. These catalysts increased the hydrogen-to-effective-carbon ratio and the proportion of volatile compounds in the WS fraction, and are suggested to promote the hydrogenation of unstable aldehydes into stable alcohols in order to increase the content of light components in the WS fraction, which contributes to the increase in the catalytic cracking yield. Iron oxides generated in situ are proposed to catalyze the isomerization of glucose into fructose and the retro-aldol condensations of sugars into low-molecular-weight compounds (C_2–C_4). As a consequence, the combined use of Fe and a metal hydrogenation catalyst favorably affects the overall pathway for the Fe-assisted HTL of cellulose to improve the yield and quality of the WS fraction due to synergistic acceleration by both the electron-transfer-type reduction by metallic Fe and hydrogenation by the metal catalyst. These results indicate the importance of increasing the yield and quality of light WS fraction components and provide a strategy for realizing economically viable biomass HTL and cracking systems. In the future, we plan to optimize the HTL conditions and to apply the findings of the present study to the HTL of real lignocellulosic biomass.

Acknowledgements

The authors gratefully acknowledge financial support from Nippon Shokubai Co., Ltd. and thank Sakai Chemical Industry Co., Ltd. for donated catalysts.

Funding

This research did not receive any specific grant from funding agencies in the public, commercial, or not-for-profit sectors.

Conflict of interest: None

References

[1] A.J. Ragauskas, C.K. Williams, B.H. Davison, G. Britovsek, J. Cairney, C.A. Eckert, W.J. Frederick, J.P. Hallett, D.J. Leak, C.L. Liotta, J.R. Mielenz, R. Murphy, R. Templer, T. Tschaplinski, The path forward for biofuels and biomaterials, Science 311 (2006) 484–489. https://doi.org/10.1126/science.1114736.

[2] P.K. Swain, L.M. Das, S.N. Naik, Biomass to liquid: A prospective challenge to research and development in 21st century, Renewable Sustainable Energy Rev. 15 (2011) 4917–4933. https://doi.org/10.1016/j.rser.2011.07.061.

[3] S. Chu, A. Majumdar, Opportunities and challenges for a sustainable energy future, Nature 488 (2012) 294–304. https://doi.org/10.1038/nature11475.

[4] P. Gallezot, Conversion of biomass to selected chemical products, Chem. Soc. Rev. 41 (2012) 1538–

1558. https://doi.org/10.1039/C1CS15147A.

[5] R.A. Sheldon, Green and sustainable manufacture of chemicals from biomass: state of the art, Green Chem. 16 (2014) 950–963. https://doi.org/10.1039/C3GC41935E.

[6] M. Su, W. Li, T. Zhang, H. S. Xin, S. Li, W. Fan, L. Ma, Production of liquid fuel intermediates from furfural via aldol condensation over Lewis acid zeolite catalysts, Catal. Sci. Technol. 7 (2017) 3555–3561. https://doi.org/10.1039/C7CY01028A.

[7] T. Zhang, W. Li, S. An, F. Huang, X. Li, J. Liu, G. Pei, Q. Liu, Efficient transformation of corn stover to furfural using p-Hydroxybenzenesulfonic acid-formaldehyde resin solid acid, Bioresour. Technol. 264 (2018) 261–267. https://doi.org/10.1016/j.biortech.2018.05.081.

[8] J. Akhtar, N.A.S. Amin, A review on process conditions for optimum bio-oil yield in hydrothermal liquefaction of biomass, Renewable Sustainable Energy Rev. 15 (2011) 1615–1624. https://doi.org/10.1016/j.rser.2010.11.054.

[9] S.S. Toor, L. Rosendahl, A. Rudolf, Hydrothermal liquefaction of biomass: A review of subcritical water technologies, Energy 36 (2011) 2328–2342. https://doi.org/10.1016/j.energy.2011.03.013.

[10] K. Tekin, S. Karagoz, S. Bektas, A review of hydrothermal biomass processing, Renewable Sustainable Energy Rev, 40 (2014) 673–687. https://doi.org/10.1016/j.rser.2014.07.216.

[11] D.C. Elliott, P. Biller, A.B. Ross, A.J. Schmidt, S.B. Jones, Hydrothermal liquefaction of biomass: Developments from batch to continuous process, Bioresour. Technol. 178 (2015) 147–156. https://doi.org/10.1016/j.biortech.2014.09.132.

[12] L. Cao, C. Zhang, H. Chen, D.C.W. Tsang, G. Luo, S. Zhang, J. Chen, Hydrothermal liquefaction of agricultural and forestry wastes: state-of-the-art review and future prospects, Bioresour. Technol. 245 (2017) 1184–1193. https://doi.org/10.1016/j.biortech.2017.08.196.

[13] A. Dimitriadis, S. Bezergianni, Hydrothermal liquefaction of various biomass and waste feedstocks for biocrude production: A state of the art review, Renewable Sustainable Energy Rev. 68 (2017) 113–125. https://doi.org/10.1016/j.rser.2016.09.120.

[14] H.A. Baloch, S. Nizamuddin, M.T.H. Siddiqui, S. Riaz, A.S. Jatoi, D.K. Dumbre, N.M. Mubarak, M.P. Srinivasan, G.J. Griffin, Recent advances in production and upgrading of bio-oil from biomass: A critical overview, J. Environ. Chem. Eng. 6 (2018) 5101–5118. https://doi.org/10.1016/j.jece.2018.07.050.

[15] A.R.K. Gollakota, N. Kishore, S. Gu, A review on hydrothermal liquefaction of biomass, Renewable Sustainable Energy Rev. 81 (2018) 1378–1392. https://doi.org/10.1016/j.rser.2017.05.178.

[16] M. Kumar, A.O. Oyedun, A. Kumar, A review on the current status of various hydrothermal technologies on biomass feedstock, Renewable Sustainable Energy Rev. 81 (2018) 1742–1770. https://doi.org/10.1016/j.rser.2017.05.270.

[17] J.P. Lange, Lignocellulose liquefaction to biocrude: A tutorial review, ChemSusChem 11 (2018) 997–1014. https://doi.org/10.1002/cssc.201702362.

[18] B. Zhang, M. von Keitz, K. Valentas, Thermochemical liquefaction of high-diversity grassland perennials, J. Anal. Appl. Pyrolysis 84 (2009) 18–24. https://doi.org/10.1016/j.jaap.2008.09.005.

[19] A. Hammerschmidt, N. Boukis, E. Hauer, U. Galla, E. Dinjus, B. Hitzmann, T. Larsen, S.D. Nygaard,

Catalytic conversion of waste biomass by hydrothermal treatment, Fuel 90 (2011) 555–562. https://doi.org/10.1016/j.fuel.2010.10.007.

[20] S. Yin, Z. Tan, Hydrothermal liquefaction of cellulose to bio-oil under acidic, neutral and alkaline conditions, Appl. Energy 92 (2012) 234–239. https://doi.org/10.1016/j.apenergy.2011.10.041.

[21] W. Shi, S. Li, H. Jin, Y. Zhao, W. Yu, The hydrothermal liquefaction of rice husk to bio-crude using metallic oxide catalysts, Energy Sources, Part A 35 (2013) 2149–2155. https://doi.org/10.1080/15567036.2012.700996.

[22] B. Meryemoğlu, A. Hasanoğlu, S. Irmak, O. Erbatur, Biofuel production by liquefaction of kenaf (*Hibiscus cannabinus* L.) biomass, Bioresour. Technol. 151 (2014) 278–283. https://doi.org/10.1016/j.biortech.2013.10.085.

[23] L. Nazari, Z. Yuan, S. Souzanchi, M.B. Ray, C. Xu, Hydrothermal liquefaction of woody biomass in hot-compressed water: Catalyst screening and comprehensive characterization of bio-crude oils, Fuel 162 (2015) 74–83. https://doi.org/10.1016/j.fuel.2015.08.055.

[24] N. Li, L. Wei, R. bibi, L. Chen, J. Liu, L. Zhang, Y. Zheng, J. Zhou, Catalytic hydrogenation of alkali lignin into bio-oil using flower-like hierarchical MoS_2-based composite catalysts, Fuel 185 (2016) 532–540. https://doi.org/10.1016/j.fuel.2016.08.001.

[25] J. Long, Y. Li, X. Zhang, L. Tang, C. Song, F. Wang, Comparative investigation on hydrothermal and alkali catalytic liquefaction of bagasse: Process efficiency and product properties, Fuel 186 (2016) 685–693. https://doi.org/10.1016/j.fuel.2016.09.016.

[26] Z. Bi, J. Zhang, E. Peterson, Z. Zhu, C. Xia, Y. Liang, T. Wiltowski, Biocrude from pretreated sorghum bagasse through catalytic hydrothermal liquefaction, Fuel 188 (2017) 112–120. https://doi.org/10.1016/j.fuel.2016.10.039.

[27] S. Cheng, L. Wei, J. Julson, P.R. Kharel, Y. Cao, Z. Gu, Catalytic liquefaction of pine sawdust for biofuel development on bifunctional Zn/HZSM-5 catalyst in supercritical ethanol, J. Anal. Appl. Pyrolysis 126 (2017) 257–266. https://doi.org/10.1016/j.jaap.2017.06.001.

[28] S.C. Yim, A.T. Quitain, S. Yusup, M. Sasaki, Y. Uemura, T. Kida, Metal oxide-catalyzed hydrothermal liquefaction of Malaysian oil palm biomass to bio-oil under supercritical condition, J. Supercrit. Fluids 120 (2017) 384–394. https://doi.org/

[29] D.D. Chen, Q.H. Ma, L.F. Wei, N.X. Li, Q.H. Shen, W. Tian, J.C. Zhou, J.Y. Long, Catalytic hydroliquefaction of rice straw for bio-oil production using Ni/CeO_2 catalysts, J. Anal. Appl. Pyrolysis 130 (2018) 169–180. https://doi.org/10.1016/j.supflu.2016.05.044.

[30] S.Y. Cheng, L. Wei, M. Rabnawaz, Catalytic liquefaction of pine sawdust and in-situ hydrogenation of bio-crude over bifunctional Co-Zn/HZSM-5 catalysts, Fuel 223 (2018) 252–260. https://doi.org/10.1016/j.fuel.2018.03.043.

[31] J.H. Lee, H. Hwang, J.W. Choi, Effects of transition metals on hydrothermal liquefaction of empty fruit bunches (EFB) for conversion to biofuel and valuable chemicals, Energy 162 (2018) 1–9. https://doi.org/10.1016/j.energy.2018.07.197.

[32] Q.H. Ma, D.D. Chen, L.F. Wei, Q.H. Shen, Z.X. Ji, Y. Chen, X.Y. Zou, C.J. Xu, J.C. Zhou, Bio-oil

production from hydrogenation liquefaction of rice straw over metal (Ni, Co, Cu)-modified CeO_2 catalysts, Energy Sources, Part A 40 (2018) 200–206. https://doi.org/10.1080/15567036.2017.1409295.

[33] R.B. Madsen, P. Biller, M.M. Jensen, J. Becker, B.B. Iversen, M. Glasius, Predicting the chemical composition of aqueous phase from hydrothermal liquefaction of model compounds and biomasses, Energy Fuels 30 (2016) 10470–10483. https://doi.org/10.1021/acs.energyfuels.6b02007.

[34] G. Tommaso, W.-T. Chen, P. Li, L. Schideman, Y. Zhang, Chemical characterization and anaerobic biodegradability of hydrothermal liquefaction aqueous products from mixed-culture wastewater algae, Bioresour. Technol. 178 (2015) 139–146. https://doi.org/10.1016/j.biortech.2014.10.011.

[35] R. Cherad, J.A. Onwudili, P. Biller, P.T. Williams, A.B. Ross, Hydrogen production from the catalytic supercritical water gasification of process water generated from hydrothermal liquefaction of microalgae, Fuel 166 (2016) 24–28. https://doi.org/10.1016/j.fuel.2015.10.088.

[36] K. Wu, M. Yang, Y. Chen, W. Pu, H. Hu, Y. Wu, Aqueous-phase ketonization of acetic acid over Zr/Mn mixed oxides, AIChE J. 63 (2017) 2958–2967. https://doi.org/10.1002/aic.15687.

[37] T.P. Vispute, H. Zhang, A. Sanna, R. Xiao, G.W. Huber, Renewable chemical commodity feedstocks from integrated catalytic processing of pyrolysis oils, Science 330 (2010) 1222–1227. https://doi.org/10.1126/science.1194218.

[38] Y. Miyata, K. Sagata, M. Hirose, Y. Yamazaki, A. Nishimura, N. Okuda, Y. Arita, Y. Hirano, Y. Kita, Fe-assisted hydrothermal liquefaction of lignocellulosic biomass for producing high-grade bio-oil, ACS Sustainable Chem. Eng. 5 (2017) 3562–3569. https://doi.org/10.1021/acssuschemeng.7b00381

[39] Y. Miyata, K. Sagata, Y. Yamazaki, H. Teramura, Y. Hirano, C. Ogino, Y. Kita, Mechanism of the Fe-assisted hydrothermal liquefaction of lignocellulosic biomass, Ind. Eng. Chem. Res. 57 (2018) 14870–14877. https://doi.org/10.1021/acs.iecr.8b03725.

[40] Y. Miyata, Y. Yamazaki, Y. Hirano, Y. Kita, Quantitative analysis of the aqueous fraction from the Fe-assisted hydrothermal liquefaction of oil palm empty fruit bunches, J. Anal. Appl. Pyrolysis 132 (2018) 72–81. https://doi.org/10.1016/j.jaap.2018.03.013.

[41] N.Y. Chen, T.F. Degnan, L.R. Koenig, Liquid fuel from carbohydrates, Chemtech 16 (1986) 506–511.

[42] H. Zhang, Y.-T. Cheng, T.P. Vispute, R. Xiao, G.W. Huber, Catalytic conversion of biomass-derived feedstocks into olefins and aromatics with ZSM-5: the hydrogen to carbon effective ratio, Energy Environ. Sci. 4 (2011) 2297–2307. https://doi.org/10.1039/C1EE01230D.

[43] Y. Hirano, Y. Kasai, K. Sagata, Y. Kita, Unique approach for transforming glucose to C3 platform chemicals using metallic iron and a Pd/C catalyst in water, Bull. Chem. Soc. Jpn. 89 (2016) 1026–1033. https://doi.org/10.1246/bcsj.20160114.

[44] Y. Hirano, K. Sagata, Y. Kita, Selective transformation of glucose into propylene glycol on Ru/C catalysts combined with ZnO under low hydrogen pressures, Appl. Catal., A 502 (2015) 1–7. https://doi.org/10.1016/j.apcata.2015.05.008.

[45] M. Möller, P. Nilges, F. Harnisch, U. Schröder, Subcritical water as reaction environment: fundamentals of hydrothermal biomass transformation, ChemSusChem, 4 (2011) 566–579. https://doi.org/10.1002/cssc.201000341.

[46] Y. Chen, X. Cao, S. Zhu, F. Tian, Y. Xu, C. Zhu, L. Dong, Synergistic hydrothermal liquefaction of wheat stalk with homogeneous and heterogeneous catalyst at low temperature, Bioresour. Technol. 278 (2019) 92–98. https://doi.org/10.1016/j.biortech.2019.01.076.

[47] B. de Caprariis, I. Bavasso, M.P. Bracciale, M. Damizia, P. De Filippis, M. Scarsella, Enhanced bio-crude yield and quality by reductive hydrothermal liquefaction of oak wood biomass: Effect of iron addition, J. Anal. Appl. Pyrolysis 139 (2019) 123–130. https://doi.org/10.1016/j.jaap.2019.01.017.

Tables

Table 1

Evaluation of WS fraction quality.

System	Elemental ratios of light WS fraction components[a]			Relative contents of light and heavy WS fraction components[b]	
	H/C	O/C	H/C_{eff}	Heavy	Light
no additive	1.60	0.65	0.30	71	29
Fe	2.00	0.72	0.56	64	36
Fe + Pd/Al_2O_3	2.33	0.50	1.33	37	63
Fe + Ru/Al_2O_3	2.24	0.49	1.25	28	72
Fe + Pt/Al_2O_3	2.21	0.51	1.19	26	74
Fe + Cu/SiO_2	2.04	0.52	0.99	47	53
Fe + Ni/kieselguhr	2.28	0.52	1.23	39	61

[a] Determined by summing of elements in each compound quantified by GC analysis.

[b] Calculated based on the carbon content of the freeze-dried crude WS fraction.

Table 2

Quality evaluation of WS fractions obtained using systems listed in Fig. 4.

System	Elemental ratios of light WS fraction components[a]			Relative contents of light and heavy WS fraction components[b]	
	H/C	O/C	H/C_{eff}	Heavy	Light
Conventional	1.60	0.65	0.30	71	29
Fe	2.00	0.72	0.56	64	36
FeO_x	1.90	0.87	0.15	78	22
Fe + Pd/Al_2O_3	2.33	0.50	1.33	37	63
Pd/Al_2O_3 + H_2[c]	1.94	0.56	0.82	48	52
FeO_x + Pd/Al_2O_3 + H_2[c]	2.07	0.49	1.09	33	67

[a] Determined by summing of elements in each compound quantified by GC analysis.

[b] Calculated based on the carbon content of the freeze-dried crude WS fraction.

[c] Initial pressure = 1.0 MPa N_2 + 1.5 MPa H_2 (i.e., the atmosphere was identical to that used for Fe-assisted HTL).

Supplementary Information

Fe-assisted hydrothermal liquefaction of cellulose: Effects of hydrogenation catalyst addition on properties of water-soluble fraction

Yoshiaki Hirano,[a,1*] Yoshinori Miyata,[a,b] Makiko Taniguchi,[a] Nami Funakoshi,[a] Yoshiko Yamazaki,[a] Chiaki Ogino,[a] and Yuichi Kita[a]

[a]*Department of Chemical Science and Engineering, Graduate School of Engineering, Kobe University, Kobe 657-8501, Japan*

[b]*Research Center, Innovation & Business Development Division, Nippon Shokubai Co., Ltd., Suita, Osaka 564-0034, Japan*

[*]Corresponding author. Tel.: +81-78-803-6512, email: hirano@phoenix.kobe-u.ac.jp

1Present address: yoshiaki_hirano@shokubai.co.jp, New Business Planning Department, Innovation & Business Development Division, Nippon Shokubai Co. Ltd., Suita, Osaka 564-0034, Japan

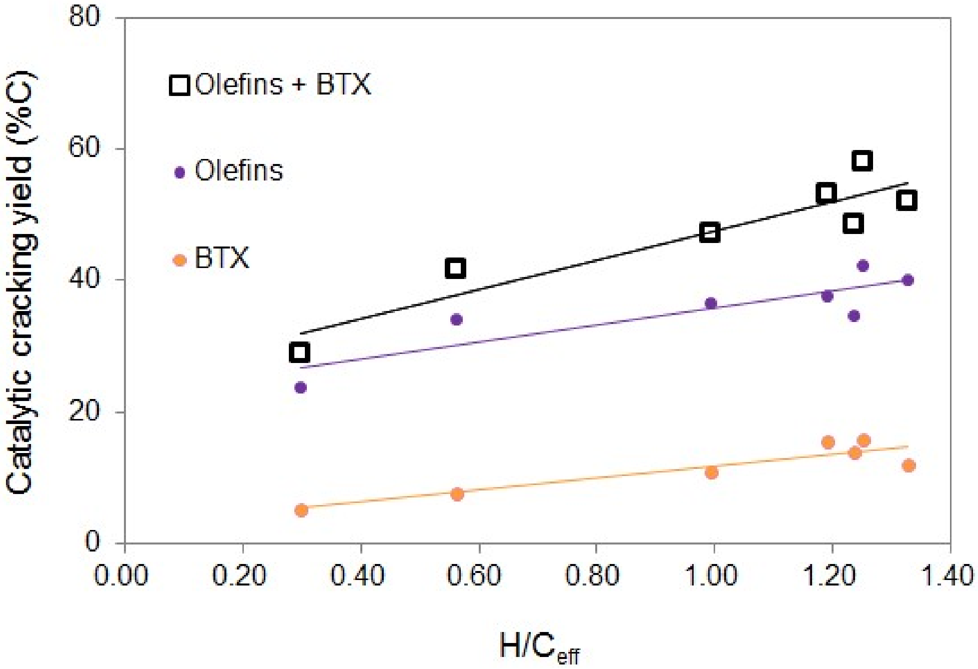

Fig. S1. Relationships between the H/Ceff ratios and catalytic cracking yields of the WS fraction on the Fe-assisted HTL of cellulose with hydrogenation catalysts.

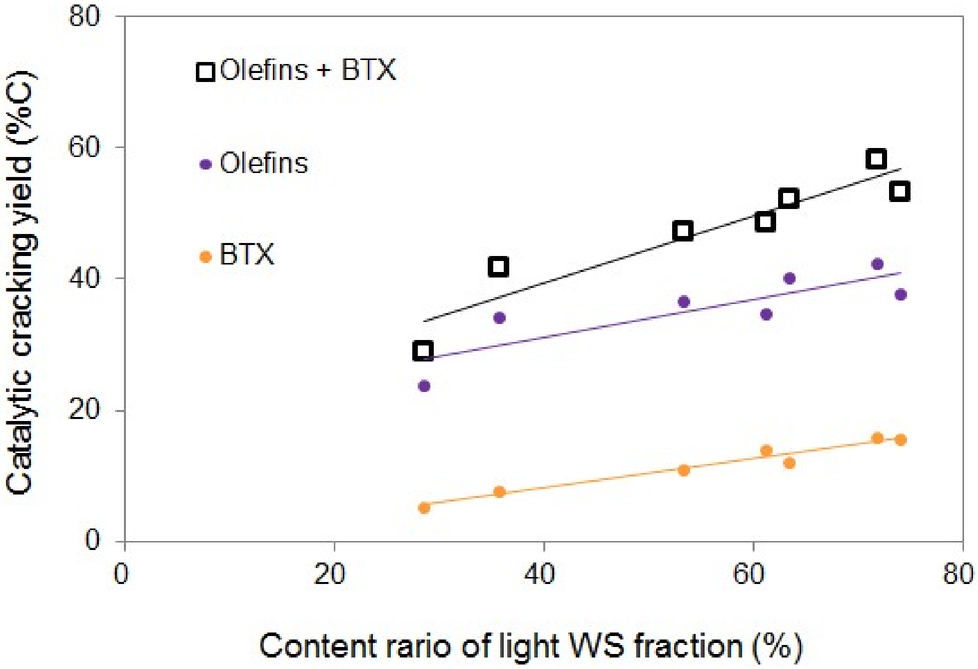

Fig. S2. Relationships between the content ratios of the light WS fractions and catalytic cracking yields of the WS fractions on the Fe-assisted HTL of cellulose with hydrogenation catalysts.

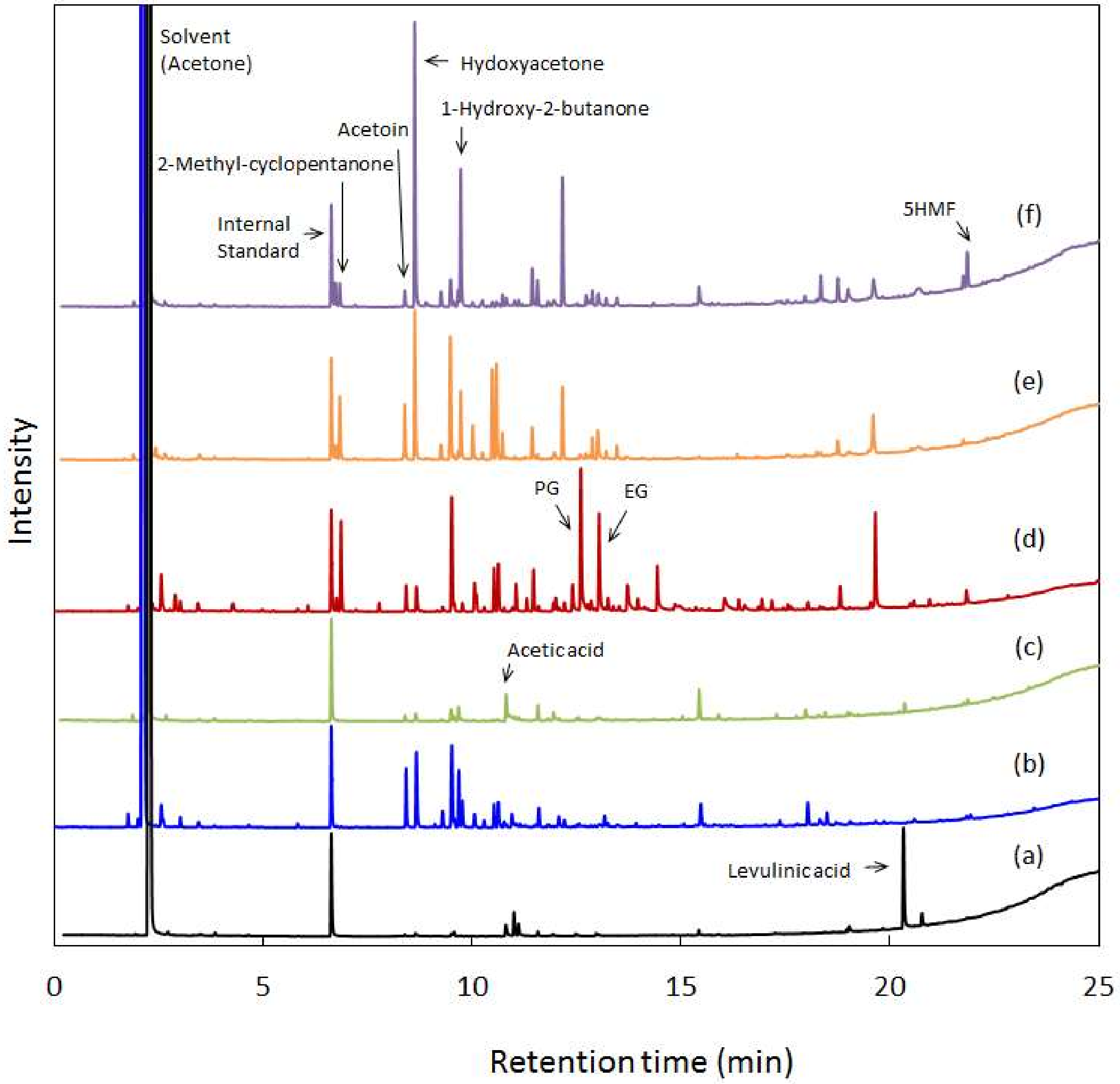

Fig. S3. GC profiles of WS fractions produced by cellulose HTL (a) with no additive and in the presence of (b) Fe, and (c) FeO_x, (d) Fe + Pd/Al_2O_3, (e) FeO_x + Pd/Al_2O_3, and (f) Pd/Al_2O_3.

Table S1. Quantitative analysis of the WS fraction obtained by cellulose HTL.

Retention time (min)	Reaction system	Yield[a] of compound (%C)					
		none	Fe	FeO_x	Fe + Pd/Al_2O_3	$Pd/Al_2O_3+H_2$	FeO_x + $Pd/Al_2O_3+H_2$
2.5	Methanol					0.3%	0.4%
2.6	2-Butanone	0.1%	0.2%	0.2%		0.0%	0.1%
2.9	Ethanol				0.7%		
3.4	2-Pentanone	0.1%	0.2%	0.1%	0.3%	0.1%	0.2%
4.2	Propanol				0.4%		0.1%
6.7	Cyclopentanone		0.1%		0.4%	0.8%	0.5%
6.7	2-Methyl-cyclopentanone		0.0%		2.6%	0.7%	2.0%
8.3	3-Hydroxy-2-butanone (acetoin)	0.1%	2.0%	0.2%	0.9%	0.6%	1.9%
8.6	1-Hydroxy-2-propanone (hydroxyacetone)	0.3%	6.0%	0.7%	2.0%	20.5%	11.2%
9.6	2-Methyl-2-cyclopenten-1-one			0.5%		0.5%	0.2%
9.7	1-Hydroxy-2-butanone		1.1%	0.1%	0.3%	4.9%	2.5%
9.9	Cyclohexanol		0.0%		0.5%		
10.2	4-Hydroxy-3-hexanone		0.2%		0.1%	0.2%	0.2%
10.5	2-Pentyl-methoxyacetate		0.8%	0.1%	1.4%	0.2%	2.8%
10.6	1-Hydroxy-2-pentanone					0.4%	0.9%
10.8	Acetic acid	0.8%	1.1%	1.7%		0.4%	
11.0	Furfural	1.0%		0.3%		0.2%	
11.2	Tetrahydro-2-furanmethanol		0.1%		1.4%	1.2%	1.0%
11.5	2,5-Hexanedione	0.2%	0.7%	0.5%	0.2%	0.8%	0.2%

11.6	2,3-Butanediol	0.1%		0.5%	0.3%		
11.9	Propanoic acid				0.5%	0.2%	0.4%
12.1	2,3-Butanediol				1.3%		
12.5	Propylene glycol (PG)		0.0%		5.9%		0.3%
12.8	1-Ethoxy-3-pentanol		0.0%		0.4%	0.3%	0.1%
13.0	Ethylene glycol (EG)		0.2%	0.1%	5.1%	0.7%	1.6%
13.0	Butanoic acid						
13.1	Butyrolactone		0.1%	0.1%	0.5%	0.3%	0.2%
13.4	1,2-Butanediol				1.7%		
14.5	1,2-Pentanediol			0.1%	0.6%		
15.4	3-Methyl-1,2-cyclopentanedione	0.2%		1.1%		0.8%	0.1%
15.7	1,2-Hexanediol				1.2%		
16.1	1,4-Butanediol				0.4%		0.1%
16.6	1,2-Cyclohexanediol				0.3%		
16.9	Cyclopentane-1,2-diol				0.3%		
17.3	Phenol		0.2%	0.1%			
17.4	Cinnamaldehyde			0.1%			
19.3	1,1'-[Ethylidenebis(oxy)]bis[2-methylpropane]		0.2%		3.7%	1.2%	1.9%
20.4	4-Oxopentanoic acid	5.1%		0.5%			
21.8	5-Hydroxymethyl-2-furaldehyde (5HMF)			0.2%		1.6%	

[a] Yields were calculated based on the carbon content of the loaded cellulose for HTL.